DOI: 10.1002/chem.200800760

Visualization of Various Supramolecular Assemblies of Oligo(*para*-phenylenevinylene)–Melamine and Perylene Bisimide

Freek J. M. Hoeben,[a] Jian Zhang,[b] Cameron C. Lee,[a] Maarten J. Pouderoijen,[a] Martin Wolffs,[a] Frank Würthner,[c] Albertus P. H. J. Schenning,*[a] E. W. Meijer,*[a] and Steven De Feyter*[b]

Abstract: A melamine derivative has been covalently equipped with two oligo(*para*-phenylenevinylene) (OPV) chromophores. This procedure yields a bifunctional molecule with two hydrogen-bonding arrays available for complementary binding to perylene bisimide derivatives. Depending on the solvent, hydrogen-bonded trimers, tetramers, and dimers on a graphite surface are observed for pure OPV–melamine by using scanning tunneling microscopy (STM). Upon the addition of perylene bisimide, linear tapes of perylene bisimide, 12-membered rosettes that consist of alternating hydrogen-bonded OPV–melamine and perylene bisimide moieties are visualized. These results provide direct evidence for the possible modes of hydrogen bonding within a supramolecular co-assembly in solution. Subsequently, the optical properties of pure OPV–melamine and co-assemblies with a perylene bisimide derivative were characterized in solution. In an apolar solvent, OPV–melamine self-assembles into chiral superstructures. Disassembly into molecularly dissolved species is reversibly controlled by concentration and temperature. Complementary hydrogen bonding to a perylene bisimide derivative in an apolar solvent yields multicomponent, π-stacked dye assemblies of enhanced stability that are characterized by fluorescence quenching of the constituent chromophores. Titration experiments reveal that a mixture of hydrogen-bonded oligomers is present in solution, rather than a single discrete assembly. The solution experiments are consistent with the STM results, which revealed various supramolecular assemblies. Our system is likely not to be optimally programmed to obtain a discrete co-assembled structure in quantitative yield.

Keywords: chirality · donor–acceptor systems · hydrogen bonds · scanning probe microscopy · self-assembly

Introduction

The design of functional π-conjugated structures for implementation in the field of organic electronics has been shown to be a promising strategy.[1] Our previous work focused on the combination of oligo(*para*-phenylenevinylene) (OPV) and perylene bisimide (PBI) dyes and yielded a variety of multicomponent supramolecular architectures based on π–π stacking and hydrogen-bonding interactions.[2] The electronic nature of the constituting OPV (p-type) and PBI (n-type) units ensured that the resulting co-assemblies were generally characterized by efficient electron transfer from the OPV to the PBI species. Eventually, such an approach may result in efficient components for solar cells by preorganizing the system for charge separation.[3] Furthermore, the quest for well-defined donor–acceptor co-assemblies yields valuable noncovalent model systems for fundamental charge-transfer studies in addition to their covalent counterparts.[4]

[a] Dr. F. J. M. Hoeben, Dr. C. C. Lee, M. J. Pouderoijen, M. Wolffs, Dr. A. P. H. J. Schenning, Prof. Dr. E. W. Meijer
Laboratory of Macromolecular and Organic Chemistry Eindhoven University of Technology
P.O. Box 513, 5600 MB Eindhoven (The Netherlands)
Fax: (+31) 40-245-1036
E-mail: a.p.h.j.schenning@tue.nl
e.w.meijer@tue.nl

[b] Dr. J. Zhang, Dr. S. De Feyter
Laboratory of Photochemistry and Spectroscopy
Institute of Nanoscale Physics and Chemistry
Katholieke Universiteit Leuven
Celestijnenlaan 200-F, 3001 Leuven (Belgium)
E-mail: steven.defeyter@chem.kuleuven.be

[c] Prof. Dr. F. Würthner
Institut für Organische Chemie
Universität Würzburg
Am Hubland, D-97074 Würzburg (Germany)

Supporting information for this article is available on the WWW under http://www.chemeurj.org/ or from the author.

Complementary hydrogen-bonding interactions are ideally suited for creating well-defined nanostructures as a result of their high specificity and directionality.[5] Pioneering studies on the melamine/barbituric (cyanuric) acid hydrogen-bonding couple by the groups of Whitesides and Reinhoudt revealed the existence of beautiful structural motifs, such as linear tapes, crinkled tapes, six-membered rosettes, and double rosettes.[6] The successful combination of synthetic accessibility and directional hydrogen bonding of both moieties has rapidly transformed this molecular recognition principle into a flourishing area of supramolecular chemistry.[7] Using a combination of complementary hydrogen bonding to melamine derivatives and π–π stacking interactions, the groups of Kimizuka[8] and Würthner[9] have formed well-defined mesoscopic assemblies of, respectively, naphthalene bisimide and PBI derivatives in methylcyclohexane (MCH). Recently, Wasielewski and co-workers showed the formation of cylindrical nanostructures that consist of hydrogen-bonded building blocks comprised of covalently attached melamine and

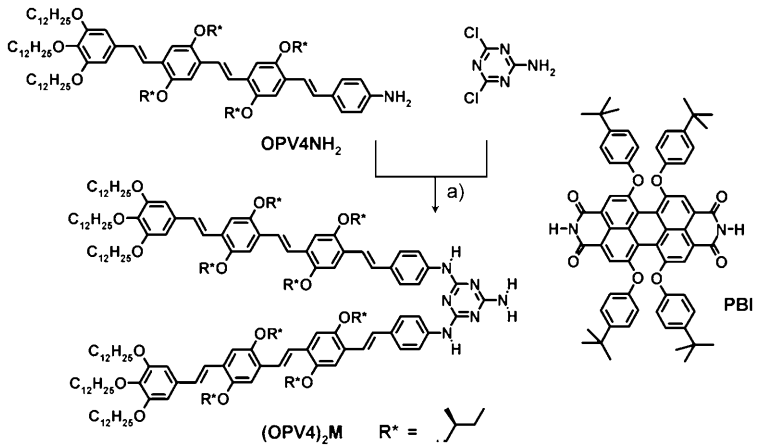

Scheme 1. Synthesis of $(OPV4)_2M$: a) diisopropylethylamine, dioxane, 100 °C, 120 h (15 %). PBI is used for co-assembly with $(OPV4)_2M$ by hydrogen bonding and π–π stacking. R* = (*S*)-2-methylbutyl.

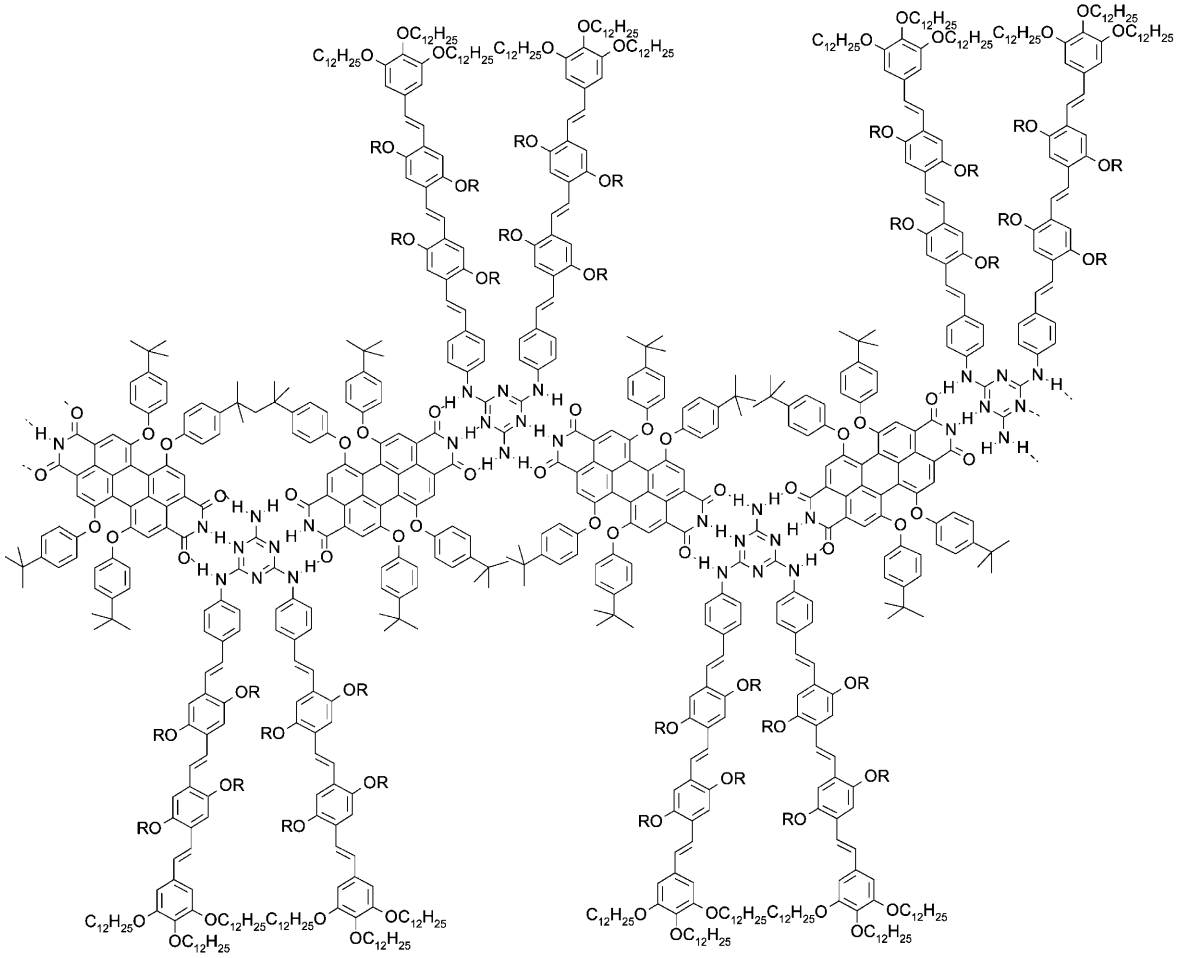

Scheme 2. Possible structures of stoichiometric co-assemblies of $(OPV4)_2M$ and PBI. A linear tapes shown here and six-membered rosette shown over.

PBI.[10] Additionally, Champness, Beton, and co-workers reported that PBI and melamine form two-dimensional hydrogen-bonded networks when the two molecules self-assemble on a silicon surface.[11] The individual cells of the thus-formed honeycomb structure were composed of 12-membered rosettes, as expected based on the geometry of the molecules. Inspired by these hydrogen-bonded systems, the covalent connection of OPV derivatives to a melamine unit is an intriguing option as this behavior may yield a new type of donor–acceptor assembly upon binding PBI derivatives.

Herein, the complexity in donor–acceptor co-assembly is enhanced by increasing the OPV density with respect to the systems studied previously.[2a,b] We explore the formation of the structural motif and subsequent self-assembly behavior at the liquid–solid interface and in solution for a novel melamine-appended OPV derivative and a complementary PBI derivative. Substitution of melamine with two OPV units results in a chromophore with two identical hydrogen-bonding arrays. This process yields bifunctional $(OPV4)_2M$ (Scheme 1), which can bind up to two PBI molecules,[12] thus giving rise to extended or cyclic structures with potentially interesting morphological and optical properties. Supramolecular donor–acceptor oligomers and cyclic hydrogen-bonded structures (Scheme 2) are observed on graphite by using scanning tunneling microscopy (STM). The ring-like structures[13] represent well-organized, densely packed chromophore ensembles. Ultimately, we show that although a number of interesting aggregate structures are observed, it is not possible to obtain a discrete supramolecular architecture in quantitative yield either in the solid state or in solution; the system, presumably, lacks a driving force to bias it towards the formation of a single aggregate type.[5]

Results and Discussion

Synthesis and characterization: Compound $(OPV4)_2M$ was readily synthesized by employing the difference in reactivity of the three electrophilic sites upon substitution of cyanuric chloride (Scheme 1). Reaction with ammonia at −5 °C re-

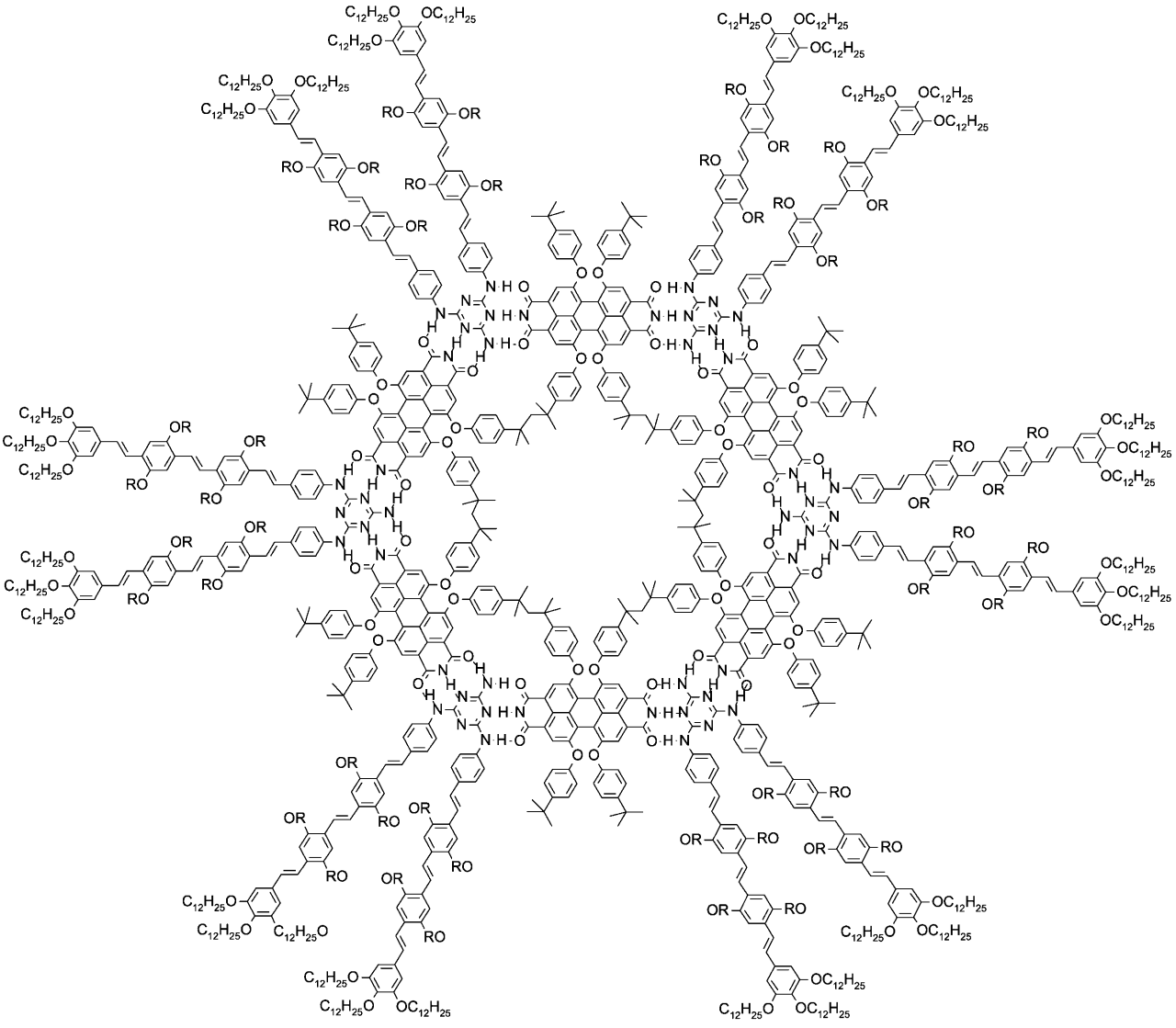

sulted in the formation of the monoaminated adduct[14] and subsequent reaction with the previously reported enantiomerically pure $OPV4NH_2$[15] yielded the desired bifunctional target compound. Pure $(OPV4)_2M$ was obtained as an orange solid in a poor yield of 15% (as a result of the relatively low reactivity of $OPV4NH_2$) after column chromatography and preparative size-exclusion chromatography; characterization was carried out with ^1H NMR, ^{13}C NMR, and IR spectroscopic and mass-spectrometric analysis. The synthesis of tetra(*tert*-butylphenoxy)perylene bisimide has been reported previously.[12]

STM analysis: As a prelude to the solution-based studies, STM analysis at the liquid–solid interface was used to obtain information on the structure of the possible co-assemblies.[16] To explore the optimum conditions under which bicomponent hydrogen-bonded supramolecular structures form, the 2D self-assembly of $(OPV4)_2M$ in 1-phenyloctane, 1,2,4-trichlorobenzene, and tetradecane was explored first. No effort was made to investigate PBI at the liquid–solid interface as this compound failed to form regular 2D lattices in previous studies.[17] The above mentioned solvents were chosen as they dissolve the compounds of interest, have low vapor pressures (a prerequisite for measurements at the liquid–solid interface without a closed cell), are electrochemically inert under the experimental conditions, and show a low tendency toward self-assembly on surfaces at room temperature.[18] In a typical experiment, a drop of solvent containing the compound(s) of interest was applied to a freshly cleaved surface of highly oriented pyrolytic graphite (HOPG). Upon spontaneous monolayer formation, STM images were acquired in the variable current mode by scanning with the STM tip immersed in the solution.

Interestingly, $(OPV4)_2M$ shows a range of different conformations and hydrogen-bonding modes at the liquid–solid interface. Typical STM images of physisorbed monolayers in the three solvents used are shown in Figure 1. The bright strips correspond to the conjugated backbone of the OPVs and indicate that the phenyl rings are adsorbed flatly on the surface. The self-assembled monolayer is disordered at the 1-phenyloctane/HOPG interface. Cyclic structures of dimers, trimers, and tetramers can be distinguished (Figure 1a; tetramer and trimer models in Figure 1d), but no preferential binding modes or conformations are obvious. Hydrogen bonding between the melamine units is likely but the precise interaction mode can not be distinguished. Domains that consist of hydrogen-bonded dimers are observed with molecules that adopt mainly a small V-shape conformation at the tetradecane/HOPG interface (Figure 1b). The point defects (missing V-shape structures) indicate that a V-shape structure corresponds to one molecule (indicated by arrows in Figure 1b).

Highly ordered 2D monolayers consisting of hydrogen-bonded dimers were obtained at the 1,2,4-trichlorobenzene/HOPG interface (Figure 1c). The molecules in the monolayers adopt a big V-shape conformation with well-separated OPV moieties. The difference in the appearance of

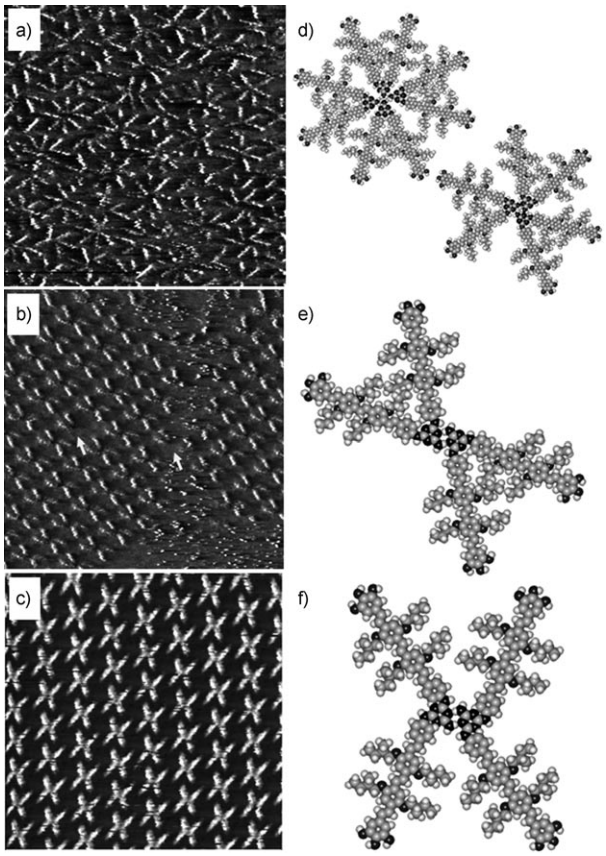

Figure 1. STM images showing monolayers of $(OPV4)_2M$ on HOPG physisorbed from a) 1-phenyloctane (image size: 40×40 nm^2, $I_{set}=0.48$ nA, $V_{set}=-0.486$ V), b) tetradecane (image size: 48.5×48.5 nm^2, $I_{set}=0.56$ nA, $V_{set}=-0.66$; the arrows indicate vacancies in the 2D lattice), and c) 1,2,4-trichlorobenzene (image size: 45.5×45.5 nm^2, $I_{set}=0.7$ nA, $V_{set}=-1.2$ V). d)–f) Tentative molecular models for the repetitive units of the self-assembled structures observed in (a)–(c), respectively.

$(OPV4)_2M$ is attributed to molecular conformational effects that most likely occur as the result of rotation around the single C–N bond that links the OPV moiety to the *s*-triazine ring. The domain sizes of the monolayers correlate to the degree of monolayer order. Thus, the well-ordered monolayers at the 1,2,4-trichlorobenzene/HOPG interface are the largest and cover areas as large as 40000 nm^2. The domains are typically smaller than 2500 nm^2 at the tetradecane/HOPG interface, and disordered regions often appear between the ordered domains. The most disordered monolayer (amorphous) is found at the 1-phenyloctane/HOPG interface. In all cases, hydrogen bonding is presumably involved in stabilizing the supramolecular structures. Because of the disorder present at the 1-phenyloctane/HOPG interface, the exact interaction mode between the melamine units is unclear. The images suggest that the melamine units interact through two hydrogen bonds at the tetradecane/HOPG and 1,2,4-trichlorobenzene/HOPG interfaces, thus leading to the formation of dimers (Figure 1e and Figure 1f).

The above-mentioned results highlight the importance of surface confinement and the solvent on the self-assembly process at the liquid–solid interface. Stacking between

solute molecules at the interface is unlikely because molecule–graphite π–π interactions are expected to overrule intermolecular π–π interactions. Furthermore, the surface itself can exert (geometrical) constraints on the ways in which the molecules adsorb through molecule–substrate interactions. In addition, solvent–substrate interactions can affect the way in which molecules initially pack onto the surface. These aspects may be the origin of the differences in the solvent-dependent surface-confined assemblies. The co-assembly of $(OPV4)_2M$ and PBI at the liquid–solid interface was also assessed by using the three solvents mentioned. To successfully image $(OPV4)_2M$/PBI complexes at the liquid–solid interface, a large excess of PBI had to be used, typically in a 1:40 ratio. This ratio is in line with our previous study on bicomponent complexes of PBI on surfaces, in which it was observed that increasing the concentration of the weakly adsorbing PBI led to an increase of heterocomplex content on the surface.[17] Despite this high ratio, no multicomponent hydrogen-bonded complexes were observed at the 1,2,4-trichlorobenzene/HOPG interface upon mixing $(OPV4)_2M$ and PBI in various ratios. Instead, only domains containing $(OPV4)_2M$ were observed, and the molecular ordering was identical to that obtained upon physisorption from a monocomponent solution.

With 1-phenyloctane and tetradecane, however, it was possible to visualize the heterocomplexes. The types of 2D self-assembled patterns formed after deposition of a drop of a solution of $(OPV4)_2M$/PBI in 1-phenyloctane on HOPG are shown in Figure 2a,b. The monolayers imaged for the mixed assemblies are largely disordered. However, occasionally 2D tape-like supramolecular oligomers (Figure 2a) and 12-membered rosettes (Figure 2b) are observed. Pairs of bright OPV rods with V-shaped conformations are visible with faint rod-like structures that link their vertices (Figure 2a). Although the features are faint, the rods could correspond to PBI molecules as the measured lengths are in good agreement with those predicted (1.13 nm; see the model in Figure 2d). Under the specific imaging conditions, cyclic structures were observed sporadically, but the full rosette proved to be very unstable and quickly became partial or disappeared. The rosettes are composed of six bright and V-shaped $(OPV4)_2M$ molecules, whereas the PBI molecules are not clearly visible (Figure 2b). The measured head-to-head distance between opposite V-shaped structures in a rosette is 3.6–3.7 nm, which corresponds nicely to the observed distance in the model presented in Figure 2e. Based on this model, the inner radius of the 12-membered supramolecular rosette is estimated to be $r = 0.89$ nm.

Similar to the situation in 1-phenyloctane, mixtures of $(OPV4)_2M$ and PBI in tetradecane gave rise to mixed monolayers. In this solvent, only half as many PBI molecules were present in the lattice, and instead of tapes and rosettes, trimers consisting of two $(OPV4)_2M$ molecules hydrogen bonded to a central PBI molecule were found (Figure 2c). The trimers are shifted with respect to each other, and as such it is not geometrically possible for another PBI molecule to link the two trimers to form a tape. As a consequence, only one of the two triple hydrogen-bonding sites of each $(OPV4)_2M$ molecule is involved in hydrogen bonding (Figure 2f).

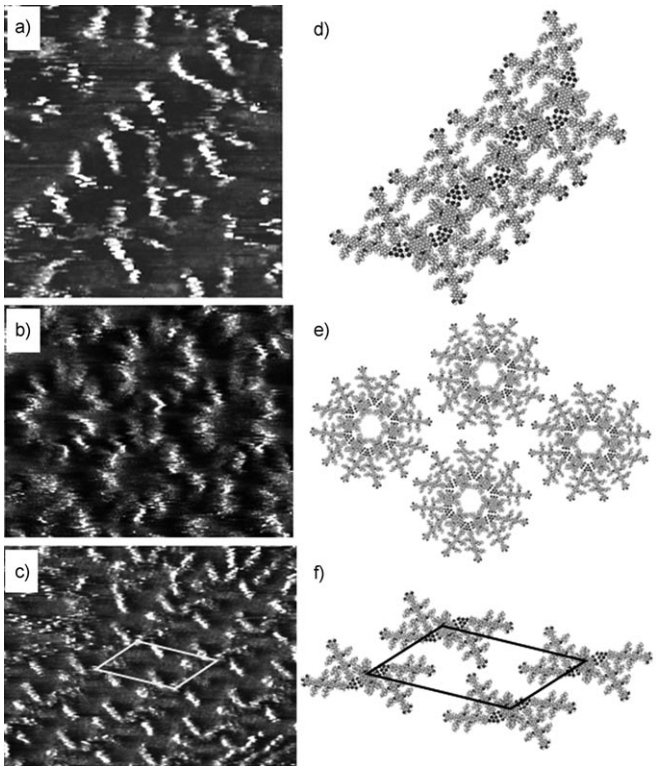

Figure 2. STM images showing co-assemblies of $(OPV4)_2M$ and PBI physisorbed on HOPG from a) 1-phenyloctane (image size: 13.0 × 13.2 nm^2, $I_{set} = 0.62$ nA, $V_{set} = -0.42$ V), b) 1-phenyloctane (image size: 12.3 × 19.7 nm^2, $I_{set} = 0.63$ nA, $V_{set} = -0.996$ V), and c) tetradecane (image size: 21.4 × 28.2 nm^2, $I_{set} = 0.46$ nA, $V_{set} = -0.402$ V; a unit cell is indicated). d)–f) The corresponding tentative models for the structures observed in (a)–(c).

Bias-dependent STM imaging was utilized to identify the PBI units on the surface.[19] At high negative sample bias (electrons tunneling from the substrate into the tip), the OPV units appear brighter than the PBI moieties because the tunneling process is more efficient through OPV than through PBI, whereas at less negative bias voltages both the OPV and PBI units are visible. Figure 3a,b are STM images obtained sequentially at the same location, thus revealing a tape-like structure at the 1-phenyloctane/HOPG interface. These images differ in the value of the negative sample bias. In Figure 3a, recorded at $V_{set} = -1.21$ V, the OPV rods appear fuzzy and no PBI molecules are visible. In Figure 3b, recorded at $V_{set} = -0.914$ V, V-shaped $(OPV4)_2M$ molecules are observed with relatively bright features that appear between them, which we attribute to PBI.

At the appropriate bias voltage ($V_{set} = -0.572$ V), the PBI molecules in partial rosettes were also revealed (Figure 4). An OPV mismatch (indicated by the arrow) appeared as a result of one of the $(OPV4)_2M$ molecules not existing in the required V-shaped conformation. In this case, it seems that rotation about the N–C bond linking one of the OPV units

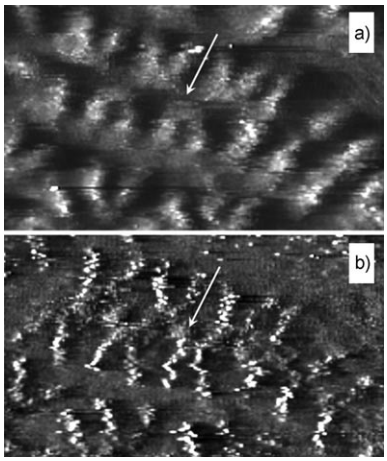

Figure 3. Bias-dependent imaging of the same area (image size: 11.3×18.7 nm^2) of an alternating tape structure of $(OPV4)_2M$ and PBI on HOPG physisorbed from 1-phenyloctane. a) $I_{set}=0.57$ nA, $V_{set}=-1.21$ V; b) $I_{set}=0.57$ nA, $V_{set}=-0.914$ V. The arrows in both images indicate identical sites, which correspond to a PBI molecule.

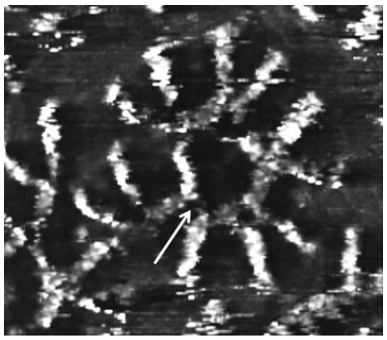

Figure 4. STM image of a partial rosette with an OPV mismatch (indicated by the arrow) on HOPG physisorbed from 1-phenyloctane (image size: 13.3×11.7 nm, $I_{set}=0.62$ nA, $V_{set}=-0.572$ V).

to the melamine core results in a conformational isomer that is not capable of completing the rosette for geometric reasons. This behavior shows that the conformational flexibility of $(OPV4)_2M$ hampers the ability of these molecules to form discrete rosette structures with PBI. Moreover, this flexibility is likely to influence the self-assembly behavior in solution as well.

Optical properties of $(OPV4)_2M$ in solution: The optical properties of pure $(OPV4)_2M$ were examined in $CHCl_3$ and MCH (Figure 5). In $CHCl_3$ (1.4×10^{-5} M), the π–π* transition of the OPV backbone is observed at $\lambda_{max}=436$ nm ($\varepsilon=1.4\times10^5$ L mol^{-1} cm^{-1}), which corresponds to the position found for previously reported similar OPV systems.[20] The compound exhibits bright fluorescence at its main emission wavelength of $\lambda_{em}=502$ nm and its first vibrational progression at $\lambda_{em}=531$ nm. Upon dissolving the molecule in MCH at an elevated concentration (7.5×10^{-5} M), the absorption maximum exhibits a hypsochromic shift to $\lambda_{max}=419$ nm accompanied by the appearance of a red-shifted shoulder at $\lambda=500$ nm. Moreover, the fluorescence is strongly quenched

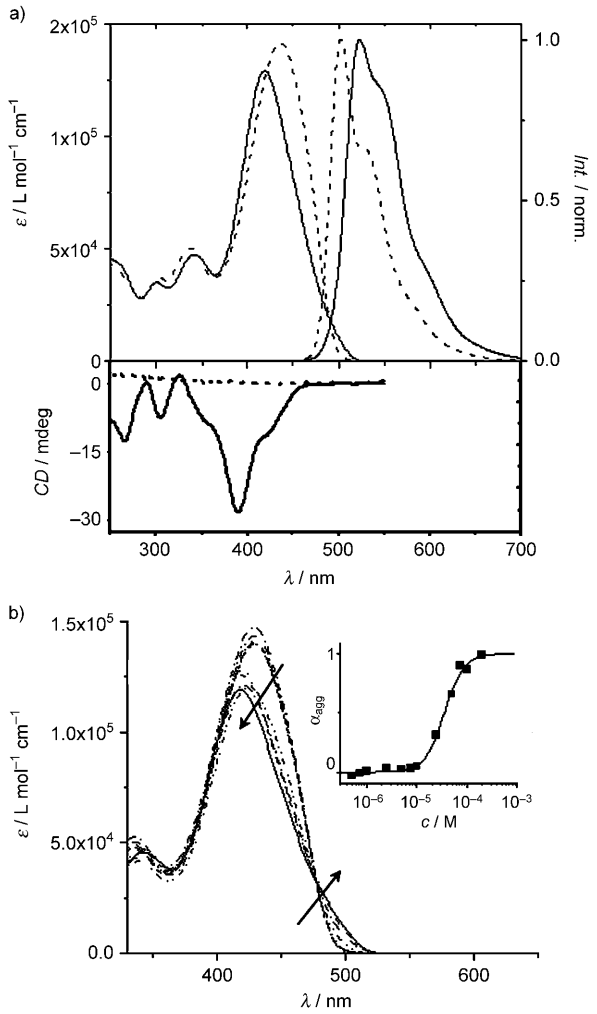

Figure 5. a) UV/vis, normalized PL, and CD spectra for $(OPV4)_2M$ in $CHCl_3$ (1.4×10^{-5} M, dashed line) and MCH (7.5×10^{-5} M, solid line), the value of λ_{exc} is the respective value of λ_{max}. b) Concentration-dependent UV/vis spectra of $(OPV4)_2M$ in MCH at room temperature; the arrows indicate increasing concentration. The inset shows the fraction of aggregated species (α_{agg}) as a function of concentration, determined by normalizing the measured absorption at $\lambda=500$ nm. Line to guide the eye. Int. = intensity.

and bathochromically shifted to $\lambda_{em}=522$ nm and $\lambda_{em}=547$ nm. These combined features are typically observed for OPV aggregation into H-type assemblies.[21] A concentration-dependent UV/vis spectroscopic study shows that the self-assembly of $(OPV4)_2M$ in MCH occurs at concentrations higher than 10^{-5} M (Figure 5b, inset).

Concomitant with the observed spectral changes upon self-assembly, a clear Cotton effect arises for $(OPV4)_2M$ that coincides with the observed UV/vis absorption bands, thus indicating that the chiral information stored in the side chains directs the aggregation process into chiral architectures. No linear dichroism was observed at these wavelengths and thus we are confident that the measured CD signal is not the result of macroscopic alignment artifacts.[22] Interestingly, the effect is largely negative, not bisignate as is usually observed for self-assembled OPVs,[20,23] thus indi-

cating a lack of exciton coupling in the $(OPV4)_2M$ structures formed. The $(OPV4)_2M$ moiety is similar in structure to a previously reported OPV4 species equipped with a diamino *s*-triazine hydrogen-bonding array (OPV4T),[24] the latter of which may be regarded a mono-OPV-substituted melamine derivative. Both $(OPV4)_2M$ and OPV4T form face-to-face packed assemblies in MCH; however, supramolecular chirality is expressed in a different fashion for both molecules. Obviously, the ability of the bifunctional molecule to rotate around the bonds centered by the nitrogen atoms that connect the OPV molecules to the *s*-triazine ring yields various chiral conformations (also see the STM data). Moreover, it is well known that the phenyl rings on a disubstituted melamine unit can be highly twisted, as found for 1:1 co-crystals with barbituric acid derivatives.[25]

Temperature-dependent UV/vis, photoluminescence (PL), and circular dichroism (CD) measurements were performed on $(OPV4)_2M$ in MCH (7.5×10^{-5} M; Figure 6). The spectra exhibited fully reversible shifts upon heating that are consistent with disassembly to a molecularly dissolved state. At temperatures above about 24 °C, the optical properties eventually saturated at values similar to those in $CHCl_3$, thus yielding evidence that the molecules are present as dissolved species. This behavior indicates relatively weak assemblies relative to the systems studied previously,[20,24] which is also revealed in the concentration-dependent measurements. The variation of the CD spectra with increasing temperature indicates that an intermediate state is present, as the shape of the spectrum completely changes during cooling (Figure 6c, inset).

Co-assemblies with PBI that display fluorescence quenching: To investigate the feasibility of mixed-assembly formation in solution, mixing experiments were performed in MCH (Figure 7). Studies were performed in dilute solution ($<10^{-5}$ M) to ensure complete solubility of each component in MCH. Upon mixing of $(OPV4)_2M$ and PBI in various ratios, distinct shifts in the UV/vis spectra occur that are generally characteristic for the co-assembly of OPV and PBI chromophores into J-type assemblies (Figure 7a,b,d).[2b] Complexation was also monitored using fluorescence spectroscopy (Figure 7c,f). After addition of one equivalent of $(OPV4)_2M$ to PBI (5.0×10^{-6} M), PBI fluorescence at $\lambda_{em}=$ 590 nm is almost completely quenched and very little OPV emission is observed (Figure 7c). OPV emission is observed for $(OPV4)_2M$/PBI ratios greater than 1:1, thus indicating that disassembled $(OPV4)_2M$ is present in solution (pure $(OPV4)_2M$ is molecularly dissolved at this concentration). Similarly, in the reverse titration experiment, $(OPV4)_2M$ fluorescence at $\lambda_{em}=491$ nm is completely quenched after the addition of one equivalent of PBI, and very little PBI emission is observed when the PBI/$(OPV4)_2M$ ratio is $\leqq$1:1 (Figure 7f). PBI emission is observed at PBI/$(OPV4)_2M$ ratios of $>$1:1, thus indicating that disassembled PBI is present in solution.

Near-complete fluorescence quenching for both chromophores in a 1:1 mixed assembly is an indication of electron

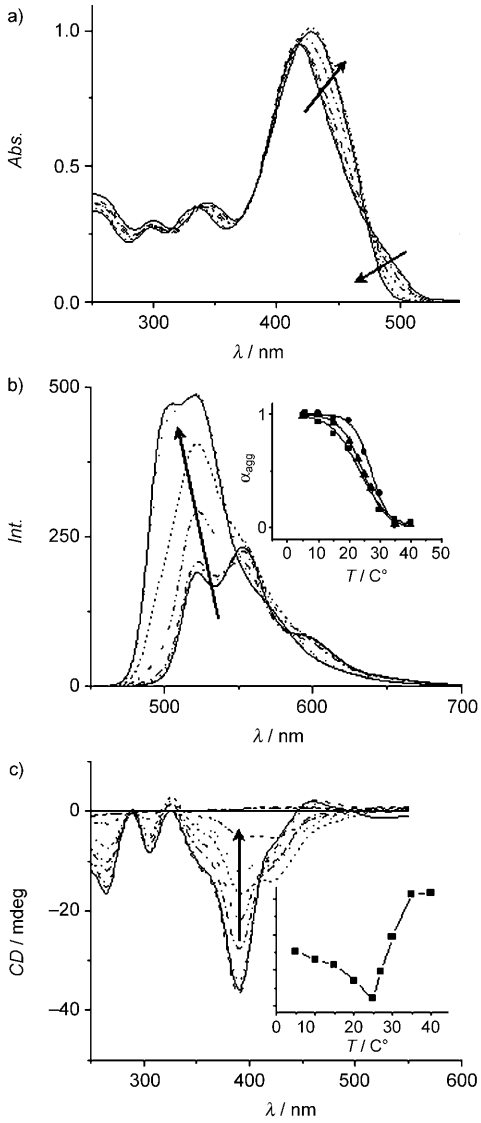

Figure 6. Temperature-dependent a) UV/vis, b) PL, and c) CD spectra for $(OPV4)_2M$ in MCH (7.5×10^{-5} M). The arrows indicate a temperature increase from 5 to 40 °C. The inset in (b) shows the fraction of aggregated species as a function of temperature, determined by normalizing the measured UV/vis ($\lambda=500$ nm, squares), PL ($\lambda=522$ nm, circles), and CD ($\lambda=$ 390 nm, triangles) data. The inset in (c) shows the CD intensity at $\lambda=$ 420 nm as a function of temperature. Lines to guide the eye. Abs. = absorption.

transfer from $(OPV4)_2M$ to PBI, as observed for closely related systems.[2b] However, we were not able to distinguish between the formation of a charge-separated state or energy transfer to a nonemissive state from femtosecond transient absorption measurements (data not shown).

The lack of fluorescence at 1:1 stoichiometries suggests that strong binding occurs between $(OPV4)_2M$ and PBI. However, if hydrogen bonding is the only intermolecular interaction responsible for the assembly of the two chromophores, full binding should not be achieved at micromolar concentrations as the association constant for triple hydrogen bonding between melamine and PBI is at the most $k=$ 10^5 M^{-1} in MCH.[9a,12] Even when the possibility of cycle for-

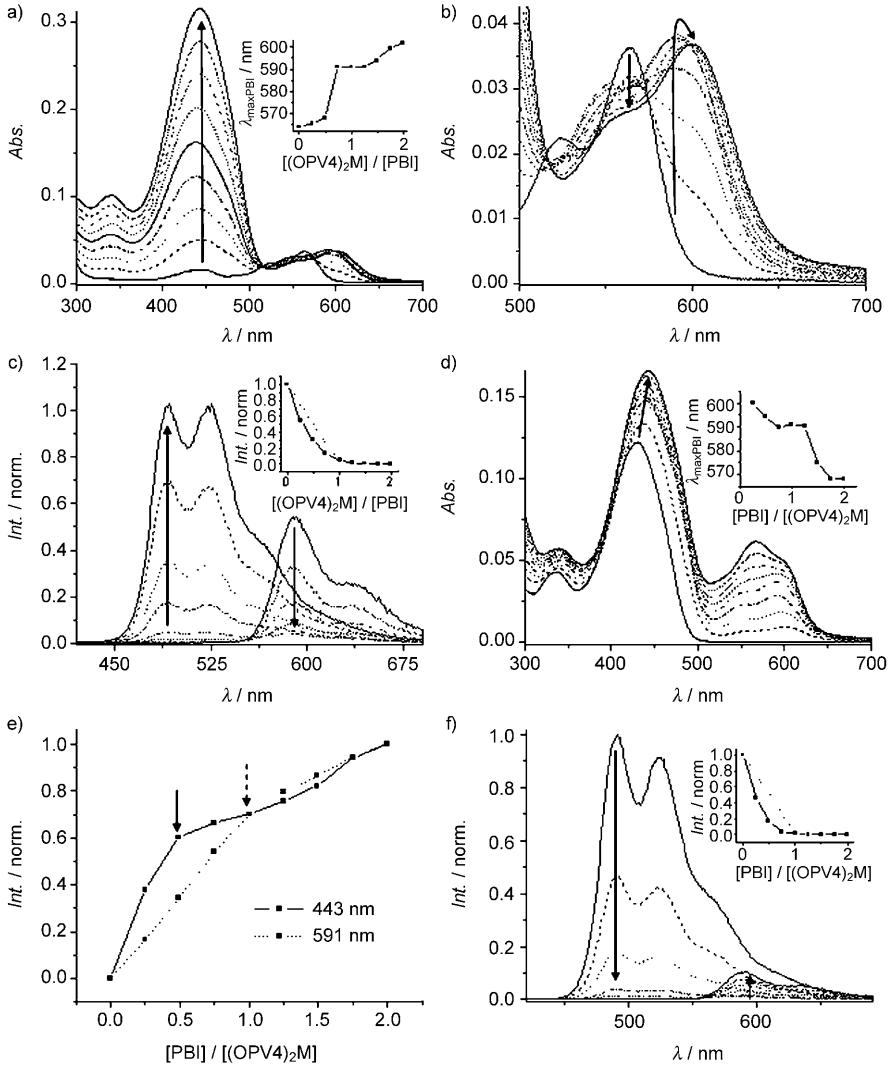

Figure 7. a,b) UV/vis and c) PL ($\lambda_{exc}=350$ nm) data showing the spectral changes upon addition of 0–2 equivalents of $(OPV4)_2M$ to a 5.0×10^{-6} M solution of PBI in MCH at room temperature; b) an enlargement of (a). d,e) UV/vis and f) PL ($\lambda_{exc}=350$ nm) data of the spectral changes upon addition of 0–2 equivalents of PBI to a 5.1×10^{-6} M solution of $(OPV4)_2M$ in MCH at room temperature; e) how the absorbances at $\lambda=443$ and 591 nm vary during the titration. The insets of (a) and (d) show how λ_{max} of PBI varies. Quenching of PBI ($\lambda_{exc}=535$ nm) and $(OPV4)_2M$ ($\lambda_{exc}=350$ nm) fluorescence is shown in the insets of (c) and (f), respectively; the dotted line in each inset demonstrates that the quenching curves are concave upward.

mation is considered,[26] rough calculations predict that there should be significant quantities of disassembled (and thus fluorescent) PBI and $(OPV4)_2M$ remaining in solution. The stronger than anticipated binding between $(OPV4)_2M$ and PBI implies that in addition to hydrogen bonding other interactions, such as π–π stacking and solvophobic effects, contribute to the overall stability of the co-assembly in MCH. A combination of hydrogen bonding and π–π stacking is consistent with the UV/vis spectral changes, and similar observations have been made in related systems.[2b,12]

Interestingly, the position of the maximum of the PBI absorption changes more than once during the titration (Figure 7a, inset). For example, $\lambda_{max}=564$ nm when $(OPV4)_2M$/PBI is 0, $\lambda_{max}=591$ nm when $(OPV4)_2M$/PBI is 0.75–1.25:1, and $\lambda_{max}=602$ nm when $(OPV4)_2M$/PBI is 2:1. These findings, plus a lack of clear isosbestic points, indicate that the structure of the most abundant PBI-containing species in solution changes more than once while varying the $(OPV4)_2M$/PBI ratio, thus suggesting that a single favored oligomeric assembly (e.g., a 12-membered rosette) does not exist.[27] A reverse titration of $(OPV4)_2M$ with PBI provided similar results (Figure 7d). Additionally, when monitoring the absorbance at a single wavelength, curves with single or multiple kinks are obtained, and the PBI/$(OPV4)_2M$ ratio at which a kink occurs depends on the chosen wavelength. For example (Figure 7e), when titrating $(OPV4)_2M$ with PBI, the OPV absorbance at $\lambda=443$ nm (mainly assembled OPV wavelength) displays a kink near 0.5 equivalents of PBI. When monitoring the PBI absorbance at $\lambda=591$ nm (assembled PBI wavelength), however, a kink is found near 1.0 equivalents of PBI. This evidence is further support for the presence of multiple-assembly stoichiometries and demonstrates that each chromophore shows a different sensitivity to changes in the aggregate structure.

Proof of the lack of a single self-assembled product is provided by the fluorescence titration experiments as well. When PBI is titrated with $(OPV4)_2M$, the PBI emission intensity versus $(OPV4)_2M$/PBI ratio curve is concave upward rather than linear, thus showing that PBI fluorescence quenching occurs faster than one would expect for the quantitative formation of only a 1:1 aggregate (Figure 7c, inset). When $(OPV4)_2M$ is titrated with PBI, again OPV fluorescence decreases faster than one would expect if a single 1:1 aggregate was being formed in a quantitative manner (Figure 7f, inset). If it is assumed that PBI or $(OPV4)_2M$ must be intimately incorporated into a co-assembly to have its fluorescence quenched, then these pieces of evidence strongly suggest that complex stoichiometries other than 1:1 are obtained with this system.

The aggregation behavior was further studied in temperature-dependent optical studies performed on a 1:1 mixture of $(OPV4)_2M$ and PBI (1.4×10^{-5} M; Figure 8). At high tem-

peratures, the spectra display features expected for molecularly dissolved $(OPV4)_2M$ and PBI. Therefore, the UV/vis spectrum is a summation of the contributions from both compounds. Upon self-assembly at lower temperatures, clear bathochromic shifts of the OPV absorption from $\lambda_{max}=$ 424 to 438 nm and the PBI absorption from $\lambda_{max}=559$ to 595 nm indicate co-assembly of the building blocks into a mixed J-type aggregate (Figure 8a).[2b] Concomitantly, the fluorescence of $(OPV4)_2M$ and PBI is completely quenched, both upon predominant OPV excitation at $\lambda_{exc}=417$ nm and selective PBI excitation at $\lambda_{exc}=568$ nm (Figure 8b). Surprisingly, a bisignate Cotton effect with a zero-crossing at $\lambda=$ 429 nm is recovered for the OPV chromophores upon co-assembly (Figure 8c). This behavior indicates that in the

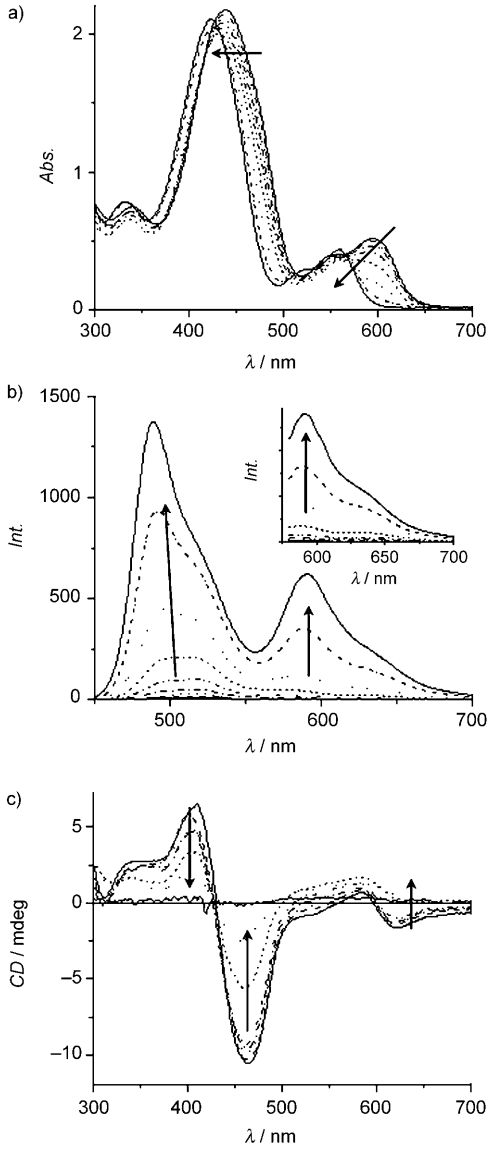

Figure 8. Temperature-dependent a) UV/vis, b) PL ($\lambda_{exc}=417$ nm), and c) CD spectra of a 1:1 mixture of $(OPV4)_2M$ with PBI in MCH (1.4×10^{-5} M). The arrows indicate a temperature increase from 10 to 90 °C. The inset in (b) shows PBI fluorescence when selectively excited at $\lambda_{exc}=$ 568 nm.

$(OPV4)_2M$/PBI hydrogen-bonded oligomers there is a left-handed, helical stacking of the OPV moieties. Also, PBI seems to exhibit a similar bisignate Cotton effect with a zero-crossing at $\lambda=597$ nm. However, the weakness of the measured signal in combination with the significant baseline drift with increasing temperature troubles a conclusive interpretation.

From the temperature-dependent UV/vis spectra, the transition from co-assemblies to molecularly dissolved species is detected at around 66 °C (1.4×10^{-5} M; Figure 8a), thus indicating enhanced stability with respect to previously studied systems.[2b] This finding was further corroborated by a concentration-dependent UV/vis study on the 1:1 $(OPV4)_2M$/PBI complex, in which the system showed little change in aggregated character when diluted from 10^{-4} M to 2.5×10^{-7} M.

The combination of hydrogen bonding and π–π stacking in the aggregates complicates the determination of a clear molecular picture. A mechanism consistent with our observations is proposed: In the absence of stacking, based on our STM results, we expect an equilibrating mixture of monomers and linear/cyclic oligomers of varying lengths. The main demands for the specific formation of cyclic hydrogen-bonded structures, namely, high binding constant and highly preorganized monomeric subunits, are both not fulfilled. We propose that steric effects that select between cyclization and linear polymerization (although the mechanistic interpretations differ)[26,28] will not play a major role in the $(OPV4)_2M$/PBI system as a consequence of the large distance that the PBI unit spans. In addition, the multiple conformational stereoisomers possible for $(OPV4)_2M$ (which result from rotation around the N–C bonds that link the OPV units to the *s*-triazine ring) and PBI (which result from interconversion between the two axially chiral forms of the highly substituted, and thus nonplanar, PBI derivative)[2b] may hinder cyclization and favor the formation of linear structures when the appropriate combination of geometries for the interacting subunits is not attained. Ultimately, we propose that these conditions give rise to an oligomer mixture of a more or less statistical nature, which is expressed both in solution (in which the oligomers are π stacked) and on HOPG (in which the oligomers are absorbed to the surface). In principle, a multitude of different structures can be envisaged (Scheme 3).

Conclusion

Co-assembly of an OPV–melamine moiety with a perylene bisimide derivative has been investigated. Bias-dependent STM studies reveal various assembly modes at the 1-phenyloctane/HOPG interface, which result in the formation of oligomeric tapes, 12-membered rosettes, and partial rosettes consisting of alternating hydrogen-bonded chromophores. Additionally, optical techniques demonstrate that OPV–melamine forms stable self-assembled heterocomplexes with perylene bisimide in solution. Titration experiments suggest

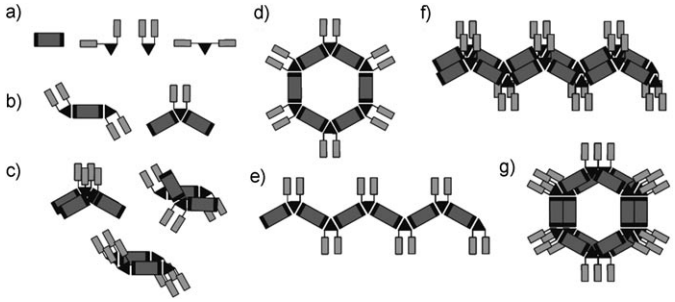

Scheme 3. a) Monomeric building blocks PBI (far left) and $(OPV4)_2M$ in three of its possible conformational isomers; b) hydrogen bonding in 1:2 and 2:1 complexes; c) stacking possibilities for 1:2 and 2:1 complexes; d) a 12-membered hydrogen-bonded rosette; e) a linear hydrogen-bonded tape; f) stacked linear hydrogen-bonded tapes; g) stacked 12-membered hydrogen-bonded rosettes. According to the spectroscopic evidence, all stacked structures should, in principle, be J-type assemblies.

that multiple aggregate stoichiometries exist for the mixed system that depend on the ratio of OPV–melamine to perylene bisimide. The origin of the disorder exhibited by the mixed system, which is expressed both on HOPG and in solution, most likely stems (amongst other factors) from the inherent conformational flexibility and lack of preorganization contained in the OPV and perylene building blocks. This behavior results in an insufficient energetic preference for one specific self-assembly mode amongst the possible cyclic and linear supramolecular motifs. It was not possible to obtain a specific discrete co-assembly in quantitative yield by adjusting common variables, such as solvent, temperature, or concentrations. Our results show that for the construction of functional multicomponent systems preorganization of the building blocks become increasingly important when using common self-assembly tools.

Experimental Section

General: ^1H and ^{13}C NMR spectra were recorded by using a 400 MHz NMR (Varian Mercury, 400 MHz for ^1H NMR and 100 MHz for ^{13}C NMR) or a 300 MHz NMR (Varian Gemini, 300 MHz for ^1H NMR and 75 MHz for ^{13}C NMR) spectrometer. In the ^1H and ^{13}C NMR spectra, chemical shifts are reported in ppm downfield from tetramethylsilane (TMS). IR spectra were recorded by using a Perkin–Elmer 1600 FT-IR. Matrix-assisted laser desorption ionization time-of-flight (MALDI-TOF) mass-spectrometric analysis was performed by using a PerSeptive Biosystems Voyager-DE PRO spectrometer. Elemental analysis was carried out by using a Perkin–Elmer 2400. UV/vis spectra were recorded by using a Perkin–Elmer Lambda 40 spectrometer. Generally, fluorescence spectra were recorded by using a Perkin–Elmer LS50B luminescence spectrometer, but the fluorescence spectra in the titration experiments were recorded by using an Edinburgh Instruments luminescence spectrometer. CD spectra were recorded by using a JASCO J-600 spectropolarimeter (sensitivity, time constant, and scan-rate were chosen appropriately).

Materials: All the solvents were of analytical reagent quality unless specified further. Dichloromethane was freshly distilled over potassium/sodium, dioxane was freshly distilled over $LiAlH_4$, and *N*,*N*-dimethylformamide (DMF) was dried over 4 Å molecular sieves. Reagents were purchased from Acros or Aldrich and were used without further purification. Bio-Beads SX-1 were obtained from Bio-Rad Laboratories. PBI,[12] 2-amino-4,6-dichloro-1,3,5-triazine,[14] and $OPV4NH_2$[15] were prepared according to reported procedures.

Synthesis of $(OPV4)_2M$: 2-Amino-4,6-dichloro-1,3,5-triazine (47 mg, 0.29 mmol) was dissolved in freshly distilled dioxane (2 mL) and the solution was heated to 40 °C. Half the amount of a solution of $OPV4NH_2$ (768 mg, 0.59 mmol, 2.1 equiv) and diisopropylethylamine (78 mg, 0.61 mmol, 2.1 equiv) in freshly distilled dioxane (16 mL) warmed to 60 °C was added dropwise. After stirring at 40 °C for 30 min, the other half of the $OPV4NH_2$ solution was added dropwise, and the reaction mixture was heated to reflux for 120 h. After cooling down to room temperature, the product was precipitated in MeOH and the orange precipitate was further purified using column chromatography on silica gel (eluent gradient: CH_2Cl_2 to 10% ethanol in CH_2Cl_2). Final purification using BioBeads SX-1 afforded the pure title compound as an orange solid (120 mg, 0.045 mmol, 15%). M.p. 140 °C; ^1H NMR ($CDCl_3$): $\delta = 0.91$ (t, 18H, $OCH_2CH_2CH_2(CH_2)_9CH_3$), 1.03 (t, 24H, $OCH_2CH(CH_3)CH_2CH_3$), 1.13 (d, 24H, $OCH_2CH(CH_3)CH_2CH_3$), 1.29–1.45 (m, 96H, $OCH_2CH_2CH_2(CH_2)_9CH_3$), 1.46–1.53 (m, 12H, $OCH_2CH_2CH_2(CH_2)_9CH_3$), 1.60–1.89 (m, 28H, $OCH_2CH(CH_3)CH_2CH_3$, $OCH_2CH_2CH_2(CH_2)_9CH_3$), 1.95–2.03 (m, 8H, $OCH_2CH(CH_3)CH_2CH_3$), 3.82–3.97 (m, 16H, $OCH_2CH(CH_3)CH_2CH_3$), 3.98–4.08 (m, 12H, $OCH_2CH_2CH_2(CH_2)_9CH_3$), 5.11 (br, 2H, NH_2), 6.77 (s, 4H, Ar*H*), 7.06 (d, 2H, C*H*=CH), 7.13 (s, 2H, Ar*H*), 7.15 (s, 2H, Ar*H*), 7.16 (d, 2H, C*H*=CH), 7.21 (s, 4H, C*H*=CH, CH=C*H*), 7.28 (br, 2H, N*H*), 7.43 (d, 2H, CH=C*H*), 7.46 (d, 2H, CH=C*H*), 7.52 (d, 4H, Ar*H*), 7.55 (s, 4H, Ar*H*), 7.62 ppm (d, 4H, Ar*H*); ^{13}C NMR ($CDCl_3$): $\delta = 11.66$, 11.73, 11.8, 14.4, 17.0, 17.11, 17.15, 22.9, 26.4, 26.62, 26.65, 29.62, 29.65, 29.70, 29.92, 29.97, 29.99, 30.01, 30.6, 32.18, 32.20, 35.2, 35.3, 35.4, 69.3, 73.8, 74.3, 74.4, 74.7, 74.8, 105.3, 109.8, 110.1, 110.7, 110.9, 120.9, 122.6, 122.8, 122.9, 127.0, 127.1, 127.2, 127.66, 127.72, 128.3, 128.8, 133.51, 133.53, 138.1, 138.4, 151.28, 151.32, 151.4, 151.5, 153.5, 164.9, 167.3 ppm; IR (UATR): $\tilde{\nu} = 3406$, 3320, 3174, 3061, 2957, 2922, 2875, 2853, 1598, 1571, 1497, 1464, 1420, 1386, 1340, 1314, 1302, 1241, 1201, 1153, 1116, 1045, 1010, 962, 916, 852, 808, 773, 722, 698 cm^{-1}; MALDI-TOF MS ($M_r = 2685.10$): m/z 2686.02 $[M]^+$.

STM analysis: All the STM experiments were performed at room temperature under ambient conditions. The STM images were obtained at the liquid–solid interface with a Discoverer scanning tunneling microscope (Topometrix Inc., Santa Barbara, CA) along with an external pulse/function generator (model HP 8111 A). The STM tips were electrochemically etched from Pt/Ir wire (80:20; diameter: 0.2 nm) in a solution of 2 N KOH/6 N NaCN in water. Prior to imaging, $(OPV4)_2M$ and PBI were dissolved in 1-phenyloctane (Aldrich) in concentrations of approximately 0.005 and 0.08 mg mL^{-1}, respectively. A drop of the solution was applied onto a freshly cleaved surface of HOPG (grade ZYB; Advanced Ceramics Inc., Cleveland, OH). The STM images were acquired in the variable current mode by scanning the STM tip immersed in solution at a negative sample bias (electrons tunnel from the sample to the tip). The measured tunneling currents are converted into a gray scale: black (white) refers to a low (high) measured tunneling current. After the successful imaging of the monolayer, an atomically resolved image of the graphite substrate was recorded at exactly the same location with identical scanning parameters except for the sample bias. The images were corrected for scanner drift by using SPIP software (Image Metrology ApS) with graphite as the calibration grid. Only images containing a small drift were used for analysis.

Titration experiments: Stock solutions of $(OPV4)_2M$ (5.1×10^{-6} M) and PBI (5.0×10^{-6} M) were prepared in spectrophotometric grade methylcyclohexane (MCH; heating was required to ensure full dissolution of the compounds in this solvent). Stock solutions of $(OPV4)_2M$ (7.0×10^{-5} M) and PBI (6.8×10^{-5} M) were also prepared in dichloromethane. PBI was titrated with $(OPV4)_2M$ as follows: the $(OPV4)_2M$ stock solution in dichloromethane (0–72.5 μL) was added to a silanized vial (Supelco) with a syringe, and the solvent was then evaporated under a stream of nitrogen. The PBI stock solution in MCH (0.5 mL) was added by syringe to the $(OPV4)_2M$ residue. The vial was capped and shaken at room temperature in the dark for 12 h. $(OPV4)_2M$ was titrated with PBI using the same method. UV/vis and photoluminescence spectra were recorded for the solutions in a 2-mm quartz cuvette at room temperature. The PL meas-

urements were collected in the front-face mode with excitation occurring at either $\lambda_{exc}=350$ nm (for OPV and PBI excitation) or $\lambda_{exc}=535$ nm (for PBI excitation).

Acknowledgement

The authors from Eindhoven thank the Council of Chemical Sciences of the Netherlands Organization for Scientific Research (NWO-CW). The authors from Leuven thank the Federal Science Policy through IUAP-V-03 and the Institute for the Promotion of Innovation by Science and Technology in Flanders (IWT). Support from the Fund for Scientific Research-Flanders (FWO) and K.U. Leuven is also appreciated. Dr. Daniela Popescu and Dr. Philippe Leclère are acknowledged for the SEM and AFM measurements, respectively.

[1] a) F. J. M. Hoeben, P. Jonkheijm, E. W. Meijer, A. P. H. J. Schenning, *Chem. Rev.* **2005**, *105*, 1491–1546; b) P. Jonkheijm, P. P. A. M. van der Schoot, A. P. H. J. Schenning, E. W. Meijer, *Science* **2006**, *313*, 80–83; c) P. Jonkheijm, P. J. K. J. van Duren, M. Kemerink, R. A. J. Janssen, A. P. H. J. Schenning, E. W. Meijer, *Macromolecules* **2006**, *39*, 784–788.

[2] a) A. P. H. J. Schenning, J. van Herrikhuyzen, P. Jonkheijm, Z. Chen, F. Würthner, E. W. Meijer, *J. Am. Chem. Soc.* **2002**, *124*, 10252–10253; b) F. Würthner, Z. Chen, F. J. M. Hoeben, P. Osswald, C. C. You, P. Jonkheijm, J. van Herrikhuyzen, A. P. H. J. Schenning, P. P. A. M. van der Schoot, E. W. Meijer, E. H. A. Beckers, S. C. J. Meskers, R. A. J. Janssen, *J. Am. Chem. Soc.* **2004**, *126*, 10611–10618; c) E. H. A. Beckers, P. Jonkheijm, A. P. H. J. Schenning, S. C. J. Meskers, R. A. J. Janssen, *ChemPhysChem* **2005**, *6*, 2029–2031; d) J. Zhang, F. J. M. Hoeben, M. J. Pouderoijen, A. P. H. J. Schenning, E. W. Meijer, F. C. De Schryver, S. De Feyter, *Chem. Eur. J.* **2006**, *12*, 9046–9055.

[3] C. H. Huang, N. D. McClenaghan, A. Kuhn, J. W. Hofstraat, D. M. Bassani, *Org. Lett.* **2005**, *7*, 3409–3412.

[4] a) E. H. A. Beckers, S. C. J. Meskers, A. P. H. J. Schenning, Z. Chen, F. Würthner, R. A. J. Janssen, *J. Phys. Chem. A* **2004**, *108*, 6933–6937; b) E. H. A. Beckers, S. C. J. Meskers, A. P. H. J. Schenning, Z. Chen, F. Würthner, P. Marsal, D. Beljonne, J. Cornil, R. A. J. Janssen, *J. Am. Chem. Soc.* **2006**, *128*, 649–657.

[5] L. J. Prins, D. N. Reinhoudt, P. Timmerman, *Angew. Chem.* **2001**, *113*, 2446–2492; *Angew. Chem. Int. Ed.* **2001**, *40*, 2382–2426.

[6] a) J. A. Zerkowski, C. T. Seto, G. M. Whitesides, *J. Am. Chem. Soc.* **1992**, *114*, 5473–5475; b) G. M. Whitesides, E. E. Simanek, J. P. Mathias, C. T. Seto, D. N. Chin, M. Mammen, D. M. Gordon, *Acc. Chem. Res.* **1995**, *28*, 37–44; c) R. H. Vreekamp, J. P. M. van Duynhoven, M. Hubert, W. Verboom, D. N. Reinhoudt, *Angew. Chem.* **1996**, *108*, 1306–1309; *Angew. Chem. Int. Ed. Engl.* **1996**, *35*, 1215–1218.

[7] a) K. Hanabusa, T. Miki, Y. Taguchi, T. Koyama, H. Shirai, *J. Chem. Soc. Chem. Commun.* **1993**, 1382–1384; b) H. Koyano, P. Bissel, K. Yoshihara, K. Ariga, T. Kunitake, *Langmuir* **1997**, *13*, 5426–5432; c) E. A. Archer, A. E. Sochia, M. J. Krische, *Chem. Eur. J.* **2001**, *7*, 2059–2065; d) P. Timmerman, L. J. Prins, *Eur. J. Org. Chem.* **2001**, 3191–3205; e) P. W. Zhu, H. Kang, A. Facchetti, G. Evmenenko, P. Dutta, T. J. Marks, *J. Am. Chem. Soc.* **2003**, *125*, 11496–11497; f) N. D. McClenaghan, C. Absalon, D. M. Bassani, *J. Am. Chem. Soc.* **2003**, *125*, 13004–13005; g) S. Keinan, M. A. Ratner, T. J. Marks, *Chem. Mater.* **2004**, *16*, 1848–1854; h) S. Yagai, M. Higashi, T. Karatsu, A. Kitamura, *Chem. Mater.* **2004**, *16*, 3582–3585; i) S. Yagai, T. Kinoshita, M. Higashi, K. Kishikawa, T. Nakanishi, T. Karatsu, A. Kitamura, *J. Am. Chem. Soc.* **2007**, *129*, 13277; j) T. Seki, S. Yagai, T. Karatsu, A. Kitamura, *J. Org. Chem.* **2008**, 39, 3328–3335; k) S. Yagai, T. Seki, T. Karatsu, A. Kitamura, F. Würthner, *Angew. Chem.* **2008**, *120*, 3415–3419; *Angew. Chem. Int. Ed.* **2008**, *47*, 3367–3371.

[8] N. Kimizuka, T. Kawasaki, K. Hirata, T. Kunitake, *J. Am. Chem. Soc.* **1995**, *117*, 6360–6361.

[9] a) F. Würthner, C. Thalacker, A. Sautter, *Adv. Mater.* **1999**, *11*, 754–758; b) C. Thalacker, F. Würthner, *Adv. Funct. Mater.* **2002**, *12*, 209–218.

[10] L. E. Sinks, B. Rybtchinski, M. Iimura, B. A. Jones, A. J. Goshe, X. B. Zuo, D. M. Tiede, X. Y. Li, M. R. Wasielewski, *Chem. Mater.* **2005**, *17*, 6295–6303.

[11] J. A. Theobald, N. S. Oxtoby, M. A. Phillips, N. R. Champness, P. H. Beton, *Nature* **2003**, *424*, 1029–1031.

[12] F. Würthner, C. Thalacker, A. Sautter, W. Schartl, W. Ibach, O. Hollricher, *Chem. Eur. J.* **2000**, *6*, 3871–3886.

[13] a) W. Kühlbrandt, *Nature* **1995**, *374*, 497–498; b) G. McDermott, S. M. Prince, A. A. Freer, A. M. Hawthornthwaite-Lawless, M. Z. Papiz, R. J. Cogdell, N. W. Isaacs, *Nature* **1995**, *374*, 517–521.

[14] a) O. Diels, *Ber. Dtsch. Chem. Ges.* **1899**, *32*, 691–702; b) H. S. Mosher, F. C. Whitmore, *J. Am. Chem. Soc.* **1945**, *67*, 662–664.

[15] E. Peeters, P. A. van Hal, S. C. J. Meskers, R. A. J. Janssen, E. W. Meijer, *Chem. Eur. J.* **2002**, *8*, 4470–4474.

[16] a) A. Marchenko, N. Katsonis, D. Fichou, C. Aubert, M. Malacria, *J. Am. Chem. Soc.* **2002**, *124*, 9998–9999; b) J. W. Zhao, K. Uosaki, *Nano Lett.* **2002**, *2*, 137–140; c) K. E. Plass, A. J. Matzger, *Chem. Commun.* **2006**, 3486–3488.

[17] S. De Feyter, A. Miura, S. Yao, Z. Chen, F. Würthner, P. Jonkheijm, A. P. H. J. Schenning, E. W. Meijer, F. C. De Schryver, *Nano Lett.* **2005**, *5*, 77–81.

[18] a) B. Venkataraman, J. J. Breen, G. W. Flynn, *J. Phys. Chem.* **1995**, *99*, 6608–6619; b) C. J. Li, Q. D. Zeng, C. Wang, L. J. Wan, S. L. Xu, C. R. Wang, C. L. Bai, *J. Phys. Chem. B* **2003**, *107*, 747–750; c) M. Lackinger, S. Griessl, W. A. Heckl, M. Hietschold, G. W. Flynn, *Langmuir* **2005**, *21*, 4984–4988; d) W. Mamdouh, H. Uji-i, J. S. Ladislaw, A. E. Dulcey, V. Percec, F. C. De Schryver, S. De Feyter, *J. Am. Chem. Soc.* **2006**, *128*, 317–325; e) L. Kampschulte, M. Lackinger, A. K. Maier, R. S. K. Kishore, S. Griessl, M. Schmittel, W. M. Heckl, *J. Phys. Chem. B* **2006**, *110*, 10829–10836; f) X. Shao, X. C. Luo, X. Q. Hu, K. Wu, *J. Phys. Chem. B* **2006**, *110*, 1288–1293.

[19] A. Miura, Z. Chen, H. Uji-i, S. De Feyter, M. Zdanowska, P. Jonkheijm, A. P. H. J. Schenning, E. W. Meijer, F. Würthner, F. C. De Schryver, *J. Am. Chem. Soc.* **2003**, *125*, 14968–14969.

[20] P. Jonkheijm, F. J. M. Hoeben, R. Kleppinger, J. van Herrikhuyzen, A. P. H. J. Schenning, E. W. Meijer, *J. Am. Chem. Soc.* **2003**, *125*, 15941–15949.

[21] E. Peeters, A. M. Ramos, S. C. J. Meskers, R. A. J. Janssen, *J. Chem. Phys.* **2000**, *112*, 9445–9454.

[22] M. Wolffs, S. J. George, Z. Tomovic, S. C. J. Meskers, A. P. H. J. Schenning, E. W. Meijer, *Angew. Chem.* **2007**, *119*, 8351–8353; *Angew. Chem. Int. Ed.* **2007**, *46*, 8203–8205.

[23] E. H. A. Beckers, Z. Chen, S. C. J. Meskers, P. Jonkheijm, A. P. H. J. Schenning, X. Q. Li, P. Osswald, F. Würthner, R. A. J. Janssen, *J. Phys. Chem. B* **2006**, *110*, 16967–16978.

[24] P. Jonkheijm, A. Miura, M. Zdanowska, F. J. M. Hoeben, S. De Feyter, A. P. H. J. Schenning, F. C. De Schryver, E. W. Meijer, *Angew. Chem.* **2004**, *116*, 76–80; *Angew. Chem. Int. Ed.* **2004**, *43*, 74–78.

[25] a) J. A. Zerkowski, C. T. Seto, D. A. Wierda, G. M. Whitesides, *J. Am. Chem. Soc.* **1990**, *112*, 9025–9026; b) J. A. Zerkowski, J. C. MacDonald, G. M. Whitesides, *Chem. Mater.* **1997**, *9*, 1933–1941.

[26] A. G. Bielejewska, C. E. Marjo, L. J. Prins, P. Timmerman, F. de Jong, D. N. Reinhoudt, *J. Am. Chem. Soc.* **2001**, *123*, 7518–7533.

[27] a) C. T. Seto, G. M. Whitesides, *J. Am. Chem. Soc.* **1993**, *115*, 905–916; b) S. Yagai, T. Nakajima, T. Karatsu, K. Saitow, A. Kitamura, *J. Am. Chem. Soc.* **2004**, *126*, 11500–11508.

[28] J. P. Mathias, E. E. Simanek, G. M. Whitesides, *J. Am. Chem. Soc.* **1994**, *116*, 4326–4340.

Received: April 22, 2008
Published online: August 1, 2008

